Multimodal piezoelectric devices optimization for energy harvesting

Giuseppe Acciani, Antonietta Dimucci* and Leonardo Lorusso
Dipartimento di Ingegneria Elettrica e dell'Informazione,
Politecnico di Bari, 70125 – Bari –Italy,
E-mail: acciani@poliba.it

ABSTRACT

The use of the piezoelectric effect to convert ambient vibration into useful electrical energy constitutes one of the most studied areas in Energy Harvesting (EH) research. This paper presents a typical cantilevered Energy Harvester device, which relates the electrical outputs to the vibration mode shape easily. The dynamic strain induced in the piezoceramic layer results in an alternating voltage output. The first six modes of frequencies and the deformation pattern of the beam are carried out basing on an eigenfrequency analysis conducted by the MEMS modules of the COMSOL Multiphysic® v3.5a to perform the Finite Element Analysis of the model. Subsequently, the piezoelectric material is cut around the inflection points to minimize the voltage cancellation effect occurring when the sign changes in the material. This study shows that the voltage produced by the device, increases in as the dimensions of the cuts vary in the piezoelectric layer. Such voltage reaches the optimum amount of piezoelectric material and cuts positioning. This proves that the optimized piezoelectric layer is 16% more efficient than the whole piezoelectric layer.

Keywords: Piezoelectric material, energy harvesting, multimodal layer

1. INTRODUCTION

Vibration-based Energy Harvesting using Piezoelectric transduction is a very attractive energy source for remote devices, the research motivation in this field is due to the reduced power requirement of small electronic components. The main advantages of piezoelectric materials in energy harvesting are their large power densities and ease of application. The piezoelectric effect, discovered by the Curie brothers in 1880, is a form of coupling between the mechanical and the electrical behaviors of ceramic and crystals belonging to certain classes, it is historically divided into two phenomena: the *direct* and the *converse* piezoelectric effects: the effect is called *Direct* when mechanically strained materials generate an electric polarization that is proportional to the applied strain; vice versa, it is called *Converse*, or *Inverse*, when the same material, subjected to an electric polarization becomes strained proportionally to the applied electric polarization. This two effects usually coexist in a piezoelectric material but, in vibration-based energy harvesting, is of particular interest only the direct piezoelectric effect.

Mechanical vibration is a potential power source which is easily accessible through Micro Electro Mechanical Systems (MEMS) technology for conversion to electrical energy. The produced energy would be useful for wireless sensors or other devices which require self-supportive power to operate. This micro renewable power energy harvesting

*Corresponding author. E-mail: dimucci@deemail.poliba.it

solution in wireless applications is a promising alternative to reduce costs and pollution, eliminating chemical batteries that can be undesirable because they tend to be bulky, have a limited life, contain a finite amount of energy, and contain chemicals [1]. A micro-electric device which generates electricity from mechanical energy, when embedded in a vibrating medium, is proposed by Williams & Yates [2], an inertial generator which uses thick-film layer of the piezoceramic Lead ZirconateTitanate (PZT) to produce electrical power is shown in [3] by Glynn-Jones *et al.*; Jeon *et al.* [4] reports a MEMS-Based power generator, called PMPG, made by athin PZT film which employs the d_{33} mode design to resonate at specific frequencies. Zheng *et al.* [5] formulate the design of energy harvesting devices under a topology optimization formulation with the aim to maximize the produced electric energy.

An appropriate material selection is also an important factor, according to previous analysis, summarized in Metwally [6], various kind of piezoelectric material are compared. In particular, fixing a mode to be utilized (d_{31}), is compared their energy conversion performance in static and eigenfrequency analysis. The comparison reveals that, the piezoelectric material PMN28 has the highest direct piezoelectricity relationship, so the considered model gave the highest electrical potential under same conditions.

According to Erturk and Inman [7], most piezoelectric energy harvesters are in form of cantilevered beams with one or two piezoceramics layers, the beam is located on a vibrating host structure and the dynamic strain induced in the piezoceramic layers results in an alternating voltage output across their electrodes.

This paper proposes an optimization of a design concept called “Multimodal energy harvesting skin” formulated by Lee and Youn [8], which uses multimodal vibration to produce energy employing piezoelectric materials.

2. ANALYTICAL FORMULATION

Several natural crystals were observed to exhibit the piezoelectric effect in the first half of the last century, in order to use them in engineering applications, the electromechanical coupling has to be sufficiently strong. In the second half of the last century, piezoelectric ceramics was developed and exhibit much larger coupling compared to natural crystals. In 1987 was published the *IEEE Standard on Piezoelectricity* [9] which contains all the forms of the **piezoelectric constitutive equations**. The Principle of conservation of energy for a linear piezoelectric continuum is:

$$\dot{U} = T_{ij}\dot{S}_{ij} + E_i\dot{D}_i \tag{2.1}$$

where U is the *Stored Energy Density*, T_{ij} is the *Stress Tensor*, S_{ij} is the *Strain Tensor*, E_i is the *Electric Field Tensor* and D_i is the *Electric Displacement Tensor*. The overdot represents differentiation respect to time.

$$H = U - E_i D_i \tag{2.2}$$

where e^H is the *Electric Enthalpy Density*. Substituting the (2.1) into the time derivative of the (2.2), results:

$$\dot{H} = T_{ij}\dot{S}_{ij} - D_i\dot{E}_i \tag{2.3}$$

so the components of Electric and Stress tensors are:

$$D_i = -\frac{\partial H}{\partial E_i}, \quad T_{ij} = \frac{\partial H}{\partial S_{ij}} \tag{2.4}$$

In linearized theory of piezoelectricity, the form of the electric enthalpy density is:

$$H = \frac{1}{2} c^E_{ijkl} S_{ij} S_{kl} - e_{kij} E_k S_{ij} - \frac{1}{2} \varepsilon^S_{ij} E_i E_j \tag{2.5}$$

Where c^E_{ijkl} is the *Elastic Constant*, e_{kij} is the *Piezoelectric Constant* and ε^S_{ij} is the *Permittivity Constant*. The superscript E and S denote that the respective constants are evaluated at constant electric field and constant strain. If δ_{ij} is the Kronecker delta, defined as:

$$\delta_{ij} \begin{cases} = 0; \text{ if } i \neq j \\ = 1; \text{ if } i = j \end{cases} \tag{2.6}$$

Using equations (2.4), (2.5) and (2.6), the *Linear Constitutive Equations for the Unbounded Piezoelectric Continuum* is given by:

$$T_{ij} = c^E_{ijkl} S_{kl} - e_{kij} E_k \tag{2.7}$$

$$D_i = e_{ikl} S_{kl} + \varepsilon^S_{ik} E_k \tag{2.8}$$

An alternative form of this equation, usually used for bounded piezoelectric media is:

$$S_{ij} = s^E_{ijkl} T_{kl} + d_{kij} E_k \tag{2.9}$$

$$D_i = d_{ikl} T_{kl} + \varepsilon^T_{ik} E_k \tag{2.10}$$

where d_{kij} is an alternative form of the *piezoelectric constant* and s^E_{ijkl} is the *elastic compliance constant*, the supersctipt T denote that the respective constants are evaluated at constant stress.

Poled piezoceramics are transversely isotropic materailas, according to IEEE Standard on Piezoelectricity [9], the plane of isotropy will be called “12-plane” or “xy-plane” and the piezoelectric material exhibits symmetry about the 3-axis or z-axis, which is the poling axis of the material. The axes orientation is shown in fig. 2.1.

Equations (2.9) and (2.10), in matrix form, become:

$$\begin{bmatrix} S \\ D \end{bmatrix} = \begin{bmatrix} s^E & d^t \\ d & \varepsilon^T \end{bmatrix} \begin{bmatrix} T \\ E \end{bmatrix} \tag{2.11}$$

The superscript t stands for the transpose. Expanding the equation (2.11), it becomes:

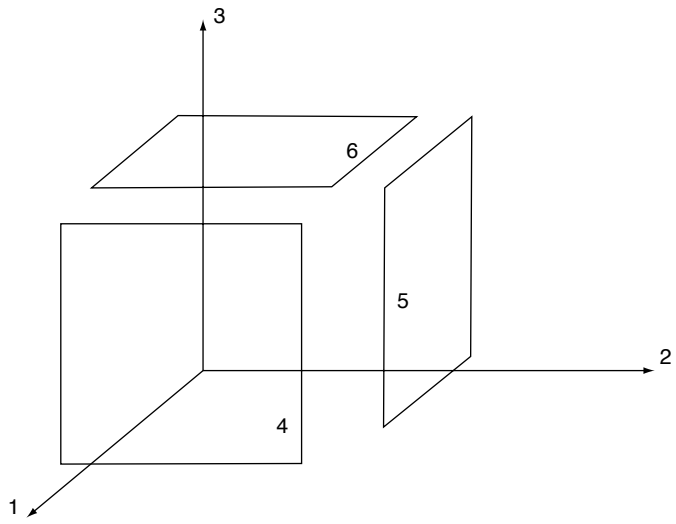

Figure 2.1

$$\begin{bmatrix} S_{11} \\ S_{22} \\ S_{33} \\ 2S_{23} \\ 2S_{13} \\ 2S_{12} \\ D_1 \\ D_2 \\ D_3 \end{bmatrix} = \begin{bmatrix} s_{11}^E & s_{12}^E & s_{13}^E & & & & 0 & 0 & d_{31} \\ s_{12}^E & s_{11}^E & s_{13}^E & & 0 & & 0 & 0 & d_{31} \\ s_{13}^E & s_{13}^E & s_{33}^E & & & & 0 & 0 & d_{33} \\ & & & s_{55}^E & 0 & 0 & 0 & d_{15} & 0 \\ & 0 & & 0 & s_{55}^E & 0 & d_{15} & 0 & 0 \\ & & & 0 & 0 & s_{66}^E & 0 & 0 & 0 \\ 0 & 0 & 0 & 0 & d_{15} & 0 & \varepsilon_{11}^T & 0 & 0 \\ 0 & 0 & 0 & d_{15} & 0 & 0 & 0 & \varepsilon_{11}^T & 0 \\ d_{31} & d_{31} & d_{33} & 0 & 0 & 0 & 0 & 0 & \varepsilon_{33}^T \end{bmatrix} \begin{bmatrix} T_{11} \\ T_{22} \\ T_{33} \\ T_{23} \\ T_{13} \\ T_{12} \\ E_1 \\ E_2 \\ E_3 \end{bmatrix} \tag{2.12}$$

For a thin beam based on the Euler-Bernoulli beam theory, the stress components other than the one-dimensional bending stress (T_{11}) are negligible:

$$T_{22} = T_{33} = T_{23} = T_{13} = T_{12} = 0$$

So, if an electrode pair covers faces perpendicular to the 3-direction, equation (2.12) becomes:

$$\begin{bmatrix} S_{11} \\ D_3 \end{bmatrix} = \begin{bmatrix} s_{11}^E & d_{31} \\ d_{31} & \varepsilon_{33}^T \end{bmatrix} \begin{bmatrix} T_{11} \\ E_3 \end{bmatrix} \tag{2.13}$$

hence the name "d_{31} *effect*". The *Stress-Electric displacement form* of the equation (2.13) is:

$$\begin{bmatrix} T_{11} \\ D_3 \end{bmatrix} = \begin{bmatrix} \tilde{c}_{11}^E & -\tilde{e}_{31} \\ \tilde{e}_{31} & \tilde{\varepsilon}_{33}^S \end{bmatrix} \begin{bmatrix} S_{11} \\ E_3 \end{bmatrix} \tag{2.14}$$

In this equation the coefficients are:

$$\tilde{c}_{11}^E = \frac{1}{s_{11}^E};\ \tilde{e}_{31} = \frac{d_{31}}{s_{11}^E};\ \tilde{\varepsilon}_{33}^S = \varepsilon_{33}^T - \frac{d_{31}^2}{s_{11}^E} \tag{2.15}$$

$\tilde{c}_{11}^E$ is the *Elasticity Constant,* $\tilde{e}_{31}$ is the *Piezoelectric Coupling Coefficient* and $\tilde{\varepsilon}_{33}^S$ is the *Dielectric Constant.*

The matrix equations relating mechanical and electrical quantities in piezoelectric media are the basis for the derivation of the Finite Element model of the cantilever beam, so the electromechanical equations can be expressed as

$$M\ddot{x} + C\dot{x} + Kx = F(t) \tag{2.16}$$

where M is the *Structural Mass Matrix*, C is the *Damping Matrix*, K is the *Stiffness Matrix* and $F(t)$ is the *Applied Force.*

If the general Equation of Motion (2.16) is considered after the application of the variational principle and Finite Element Discretization [10], the **Coupled Finite Element Matrix Equation** is:

$$\begin{bmatrix} M & 0 \\ 0 & 0 \end{bmatrix} \begin{bmatrix} \{\ddot{x}\} \\ \{\ddot{V}\} \end{bmatrix} + \begin{bmatrix} C & 0 \\ 0 & 0 \end{bmatrix} \begin{bmatrix} \{\dot{x}\} \\ \{\dot{V}\} \end{bmatrix} + \begin{bmatrix} K & K^z \\ K^{z^T} & K^d \end{bmatrix} v \begin{bmatrix} \{x\} \\ \{V\} \end{bmatrix} = \begin{bmatrix} \{F\} \\ \{L\} \end{bmatrix} \tag{2.17}$$

In the equation (2.17), K^z is the *Piezoelectric Coupling Matrix,* K^d is the *Dielectric Conductivity Matrix,* $\{x\}$ is the *Displacement Vector,* $\{V\}$ the *Voltage Vector,* $\{F\}$ is the *Structural Load Vector* and $\{L\}$ is the *Electrical Load Vector.* In our study $\{L\} = 0$.

The vibration frequency is the same in all the points of the beam so, if the Displacement, the Voltage and the Force vectors are expressed in the form:

$$\begin{aligned} \{x\} &= \{x_m\}e^{i(\varphi+\omega t)} = \{x_m(\cos\varphi + \text{isen}\varphi)\}e^{i\omega t} = \{\{x_r\} + i\{x_i\}\}e^{i\omega t} \\ \{V\} &= \{V_m\}e^{i(\varphi+\omega t)} = \{V_m(\cos\varphi + \text{isen}\varphi)\}e^{i\omega t} = \{\{V_r\} + i\{V_i\}\}e^{i\omega t} \\ \{F\} &= \{F_m\}e^{i(\varphi+\omega t)} = \{F_m(\cos\varphi + \text{isen}\varphi)\}e^{i\omega t} = \{\{F_r\} + i\{F_i\}\}e^{i\omega t} \end{aligned} \tag{2.18}$$

substituting the equations (2.18) in the equation (2.17) and cancelling $e^{i\omega t}$, the Matrix Equation is:

$$\left[-\omega^2 \begin{bmatrix} M & 0 \\ 0 & 0 \end{bmatrix} + i\omega \begin{bmatrix} C & 0 \\ 0 & 0 \end{bmatrix} \begin{bmatrix} \{\dot{x}\} \\ \{\dot{V}\} \end{bmatrix} + \begin{bmatrix} K & K^z \\ K^{z^T} & K^d \end{bmatrix} \right] \begin{bmatrix} \{x_r\} + i\{x_i\} \\ \{V_r\} + i\{V_i\} \end{bmatrix} = \begin{bmatrix} \{F_r\} + i\{F_i\} \\ 0 \end{bmatrix} \tag{2.19}$$

According to the theory of mechanical finite elements, the matrices and the vectors

describing the whole mesh (2.19) result from assembling the vectors and matrices of the single elements of which the mesh is composed. The solution of the (2.19) yields the mechanical displacement vector $\{x\}$ and the Voltage vector $\{V\}$ in the piezoelectric medium. The two vectors are coupled by the Piezoelectric coupling matrix K^z. After solving the equation, the complex electrical potential and the displacement can be expressed in the form:

$$\{V_r\} + i\{V_i\} = V_m(\cos\varphi + \text{isen}\varphi) \rightarrow V_m = \sqrt{V_r^2 + V_i^2}\,;\ \varphi(V) = \tan^{-1}\left(\frac{V_i}{V_r}\right) \tag{2.20}$$

$$\{x_r\} + i\{x_i\} = x_m(\cos\varphi + \text{isen}\varphi) \rightarrow x_m = \sqrt{x_r^2 + x_i^2}\,;\quad \varphi(x) = \tan^{-1}\left(\frac{x_i}{x_r}\right) \tag{2.21}$$

3. DESIGN AND OPTIMIZATION OF THE DEVICE

In order to obtain analytical expressions, mixing the Euler-Bernoulli beam theory with the piezoelectric constitutive equation, is easily to obtain the Electric Displacement to relate the electrical outputs to the vibration mode shape. So the studied Energy Harvesting Device, is a cantilevered beam. The design process consists of a first Design and Analysis step, to characterize the device and its behavior when a load (static and vibrating) is applied, in order to detect the inflection lines by Voltage phase angle ($\varphi(V)$) at the top surface of the piezoelectric layer; the second step consists in the optimization of the piezoelectric layer to maximize the power generation of the Energy Harvester by removing material near the inflection lines [7–8].

3.1. DESIGN

The aim of the presented study is the optimization of an Energy Harvesting device optimizing the design of the piezoelectric layer, allowing to maximize the voltage generation, by means of the d_{31} effect. To solve the model, is used COMSOL Multiphysic® v3.5a, basing on the *Finite Element Method*, the software runs the Finite Element Analysis together with adaptive meshing and error control using a variety of numerical solvers.The Energy Harvesting device is shown in fig. 3.1 and consists of two layers characterized by the following dimensions: length = 31 mm, width = 9.5 mm, height of the bottom layer of stainless steelequal to 0.05 mm and height of the top layer of piezoelectric material PMN28 equal to 0.127 mm.

The Piezoelectric Material properties are defined in the *Stress-Electric displacement form* of the equation (2.12), in which are specified:

✓ The *Elasticity Matrix:*

$$C^E = \begin{bmatrix} 7.09e^{10} & 5.77e^{10} & 7.14e^{10} & 0 & 0 & 0 \\ 5.77e^{10} & 7.09e^{10} & 7.14e^{10} & 0 & 0 & 0 \\ 7.14e^{10} & 7.14e^{10} & 1.07e^{11} & 0 & 0 & 0 \\ 0 & 0 & 0 & 6.67e^{10} & 0 & 0 \\ 0 & 0 & 0 & 0 & 6.67e^{10} & 0 \\ 0 & 0 & 0 & 0 & 0 & 3.45e^{10} \end{bmatrix} Pa$$

✓ The *Piezoelectric Coupling Matrix:*

$$e = \begin{bmatrix} 0 & 0 & 0 & 0 & 17.06667 & 0 \\ 0 & 0 & 0 & 17.06667 & 0 & 0 \\ 8.028571 & 8.028571 & 39.39286 & 0 & 0 & 0 \end{bmatrix} C/_{m^2}$$

✓ The *Dielectric Matrix:*

$$\varepsilon = \begin{bmatrix} 3631 & 0 & 0 \\ 0 & 3631 & 0 \\ 0 & 0 & 476 \end{bmatrix}$$

✓ The *Density:* $\rho = 7690\ {}^{kg}/_{m^3}$

The Steel properties for the bottom layer are well note: *Density is* $\rho = 7850\ {}^{kg}/_{m^3}$, *Young's Modulus* is $Y = 180 \infty 10^9\ {}^{N}/_{m^2}$.

There are two sets of boundary conditions: the *Mechanical Conditions* which constrain the two vertical surfaces on the left side of the beam with zero movement, while all other are

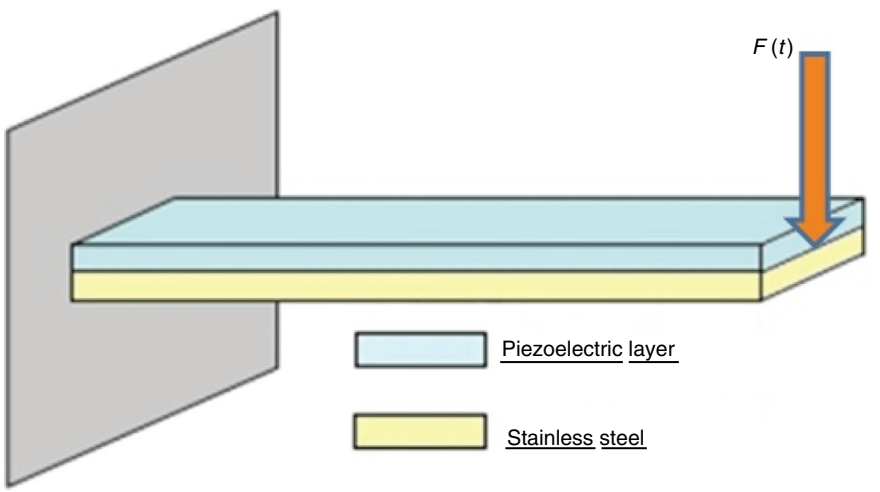

Figure 3.1

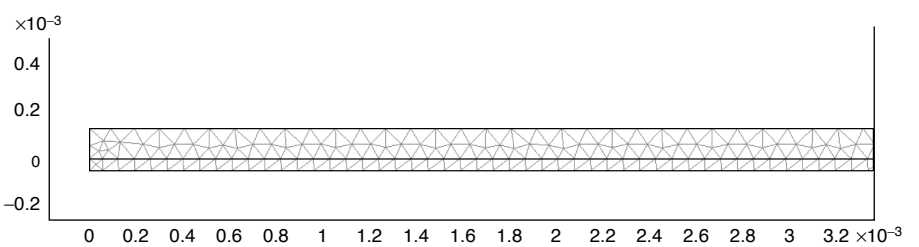

Figure 3.2

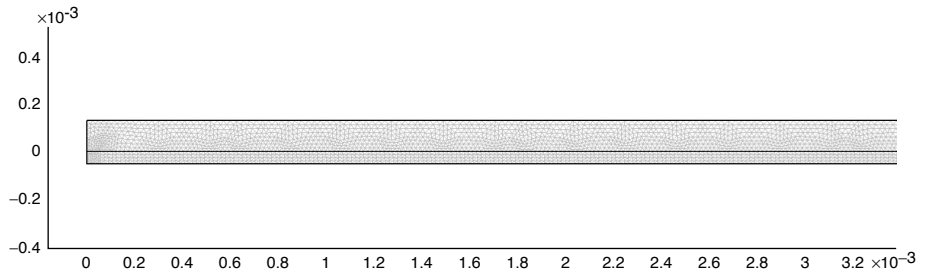

Figure 3.3

free and the *Electrical Conditions* that set the bottom surface of the piezoelectric layer as Ground and top as Zero Charge. The *External Load* $F(t) = 10e^{4\ N/m^2}$ is applied to the beam's free end in the –y direction, as shown in fig. 3.1.

Initially the cantilever beam is meshed at 2518 elements and 15539 degrees of freedom by using the Standard meshing tool of the COMSOL Multiphysic®, in fig. 3.2 is shown a portion of the beam to view the mesh density.

As the mesh density increases, the final result improves, especially in the eigenfrequency analysis; the optimal mesh density is found by gradually increasing the mesh density until it reaches a point where the result improvement is no more appreciable. In our case of study, the *optimal mesh density* results at 40288 elements and 222.035 degrees of freedom. The portion of the beam at this mesh density is shown in fig. 3.3.

3.2. STATIC ANALYSIS

The static analysis of the device is used to find the position and the magnitude of the maximum strain, stress and electrical potential on the beam, applying a static load to the beam's free end. It results a deflection in the direction of the applied load and the maximum

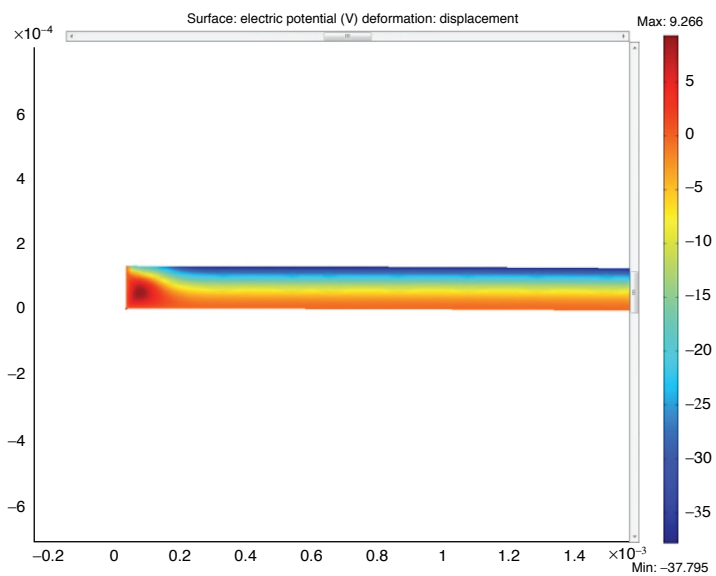

Figure 3.4

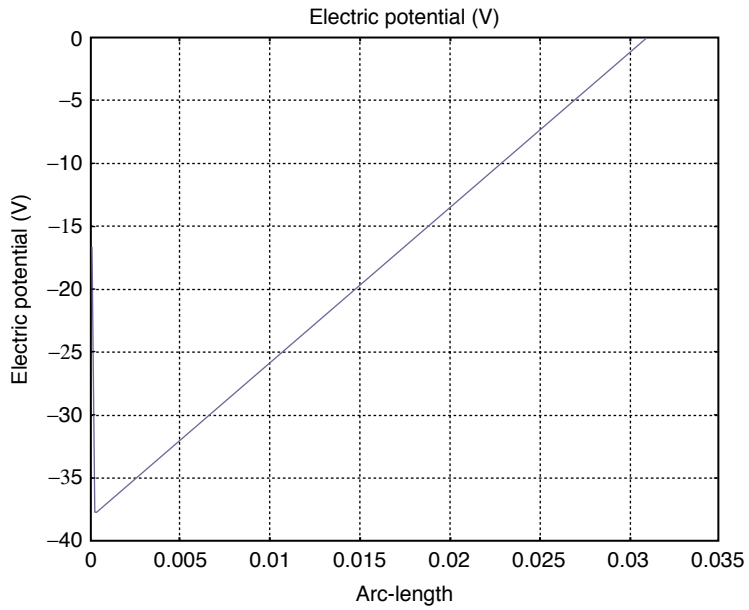

Figure 3.5

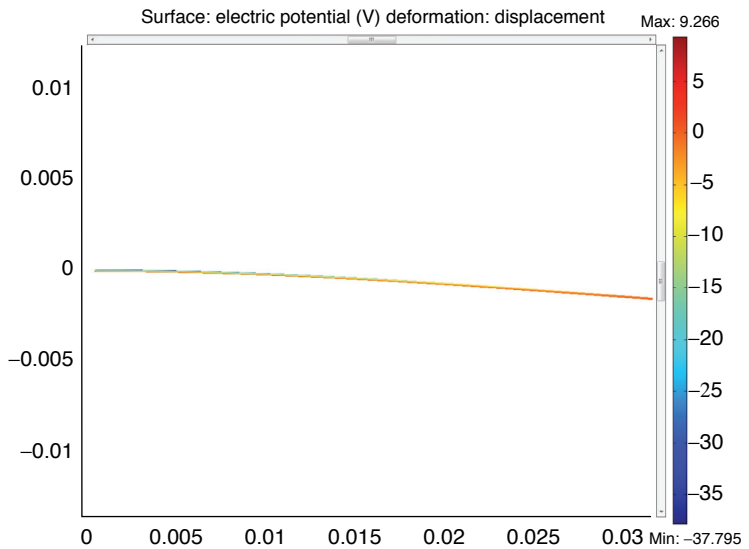

Figure 3.6

displacement is recorded at the beam's free end and is near $5.521e^{-3}$ mm. The maximum strain, stress and, subsequently, the maximum electrical potential can be observed at the beam fixed endas shown in particular in Fig. 3.4 and globally in Fig. 3.5 and 3.6. The values are shown in detail in the Table 3.1

Table 3.1

	Displacement (mm)	Maximum strain	Stress (MPa)	Maximum electrical potential (V)	Minimum electrical potential (V)
PMN28	5.13e-3	4.79e-3	118.7	9.266	–37.795

Table 3.2

	Mode 1		Mode 2		Mode 3	
Eigenfrequency (Hz)	75.130023		471.468972		1319.997455	
Position (m)	–		0.01636		0.0095	0.02196
Max. and Min. Voltage (V)	9.597	–1.708	7.109	–9.09	8.704	–6.497

3.3. EIGENFREQUENCY ANALYSIS

Afterwards the first six modes of frequencies and the deformation pattern of the beam are carried out using the eigenfrequency analysis. For modal vibrations, the *Curvature Eigenfunction* is the second derivative of the *Displacement Eigenfunction*, the frequency parameters and the positions of the strain nodes for a uniform Euler-Bernoulli beam with clamped-free boundary conditions, are easily computed using the Eigenfrequency Analysis of the COMSOL Multiphysic® and can be used to predict the *Undamped Natural Frequencies* of the device. The values founded for each mode frequency are used to find the *Inflection Point Positions,* Eigenfrequency and position along the beam are summarized in Table 3.2.

In Fig. 3.7–3.10 are shown, for each eigenfrequency, the Electric Potentials in function of the deformation shape.

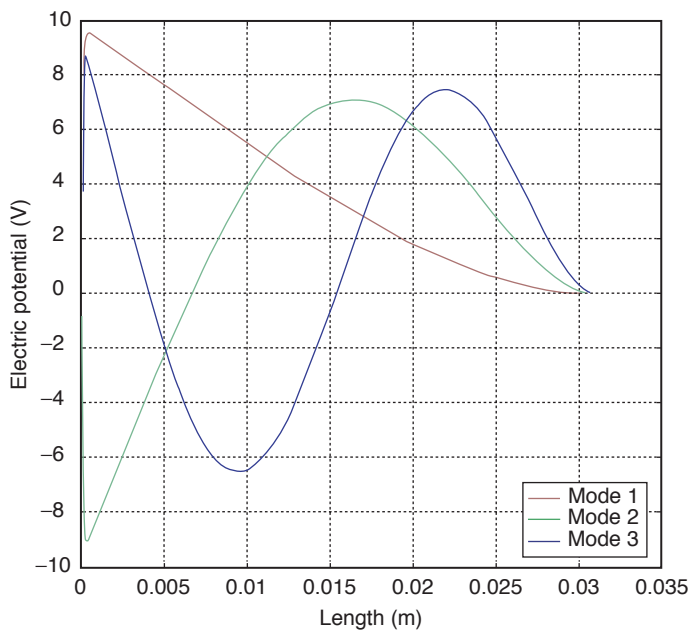

Figure 3.7

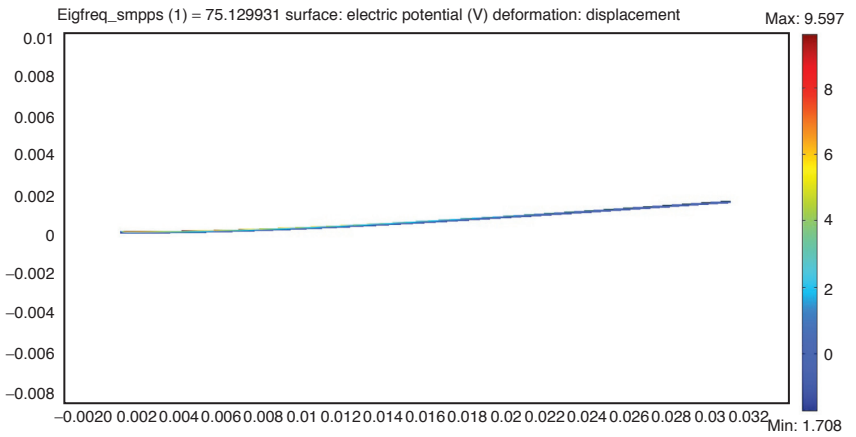

Figure 3.8

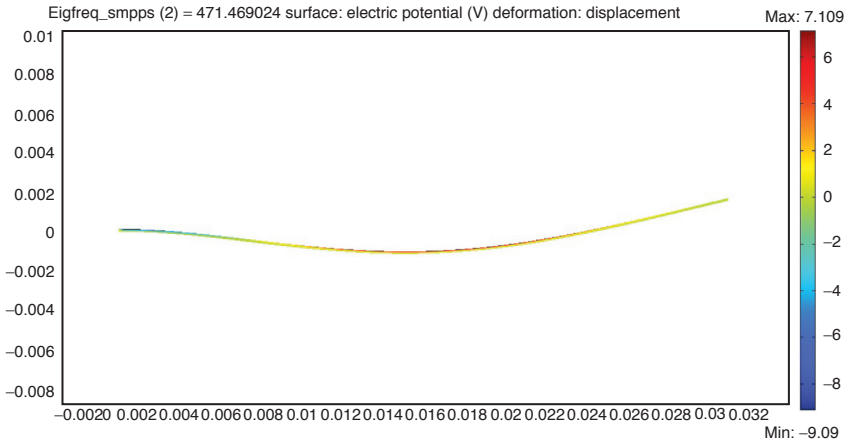

Figure 3.9

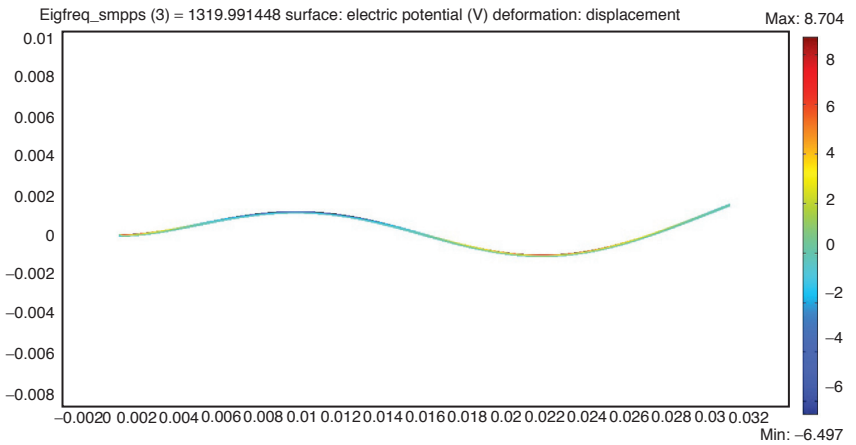

Figure 3.10

The analysis of the first three vibration modes of the cantilever beam, shows that inflections points are present since the second vibration mode and for the *n*th mode there are (*n*-1) inflection points. For a cantilevered beam without strain nodes, the only vibration mode is the fundamental. This preliminary analysis of the vibration modes has been used for the optimization of the Energy Harvesting device.

3.4. OPTIMIZATION

According to the design of a Multimodal EH Skin proposed by Lee and Youn [2], and the theories that can be found in Erturk and Inman [7], the piezoelectric material has to be cut around the inflection points to avoid the voltage cancellation effect occurring when the sign changes in the material. In the works cited above, this technique was useful in the electrodes positioning of the energy harvesting device, avoiding the inflection lines. In this study, the attention was focused to the *Optimal Distribution Of The Piezoelectric Material*, starting from the case of continuum piezoelectric layer, as shown in previous paragraphs,until the optimal material distribution is reached with the aim to maximize the Voltage Generation of the Energy Harvester.

The optimization have been considered only for the first tree modes of frequencies due to the small size of the device. For the reason explained previously, there are three cuts in the bottom piezoelectric layer of the cantilevered beam: one cut in the material corresponding to the inflection point of the mode 2, and two cuts corresponding to the inflection points of the mode 3. The material is removed symmetrically around the positions corresponding to the inflection point:

- to avoid cancellation from the *Second Vibration Mode*, positioned in $x = 0.01636$ m, the regions to cover with piezoelectric material has to be $0 \text{ m} \le x < 0.01636$ m and $0.01636 \text{ m} < x \le 0.031$ m*;*
- to avoid cancellation from the *Third Vibration Mode*, positioned in $x_1 = 0.0095$ m and $x_2 = 0.02196$ m, the regions to cover with piezoelectric material has to be $0 \text{ m} \le x < 0.0095$ m, $0.0095 \text{ m} < x < 0.02196$ m and $0.02196 \text{ m} < x \le 0.031$ m.

The piezoelectric layer of the beam, in the final configuration, has three cuts near the points x_1, x_2, and x_3 and four regions covered with piezoelectric material, as shown in Fig. 3.11(b). The amount of removed material near the inflection points to maximize the Voltage Generation is varied to reach the optimum configuration as shown in Fig. 3.11(b-c-d).

Initially, the optimization for second and third vibration mode are conducted separately, and after are simulated together. In the case of the second mode, already removing an amount of 1% of the total piezoelectric material of the layer near the inflection point, the device shows an increase of about 2V in the electrical potential difference (ΔV). The *Optimum* amount of removed material, has been found for a removal of material that is the 4% *of the total* piezoelectric layer. The trend of the voltage in the second vibration mode, considering

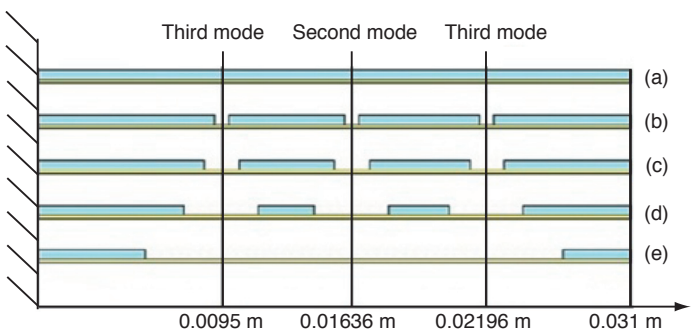

Figure 3.11

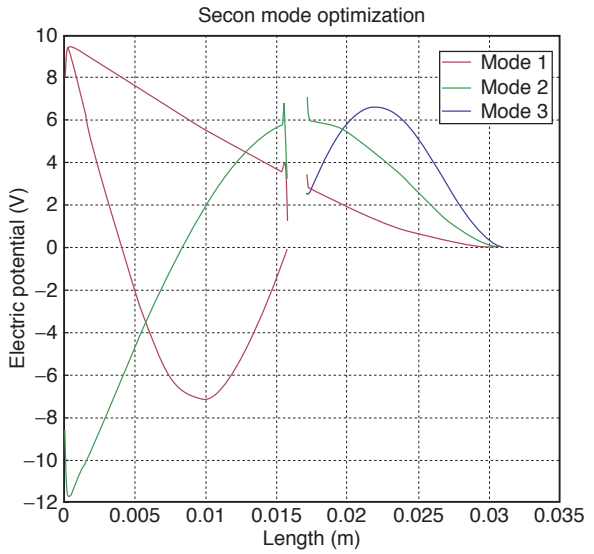

Figure 3.12

the optimum configuration is shown in Fig. 3.12 and shows an increase of about 2, 7V in the electrical potential difference (ΔV) which increases from 16,22V of the continuous distribution to 18,94V. Increasing the amount of removed material, the ΔV decreases.

For the third mode, removing an amount of 1% of the total piezoelectric material of the bottm layer near the two inflection points, the device shows an increase of the electrical potential difference (ΔV) that is about 2,1V. The optimum amount of removed material, has been found for a removal that is the 14% of the total piezoelectric layer (7% for each inflection point). The trend of the voltage in the third vibration mode, considering the optimum configuration is shown in Fig. 3.13 and shows that the electrical potential difference (ΔV) increases from 15,24V to 20,48V.

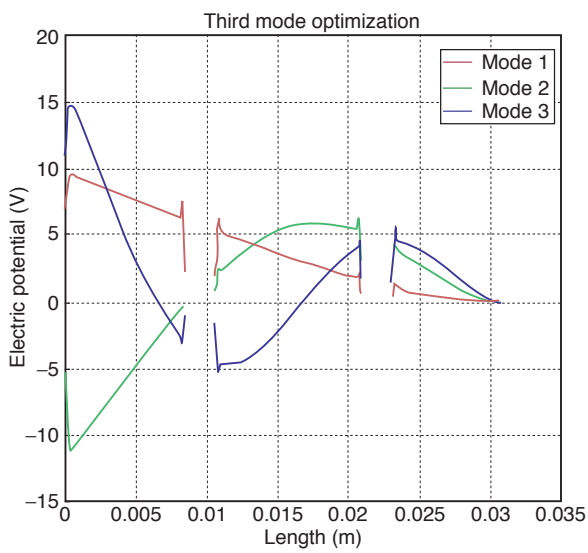

Figure 3.13

Table 3.3

	[m]	[%]	mode 1			mode 2			mode 3			Global
	Width removed material	% removed material	f [Hz]	Vmax [V]	ΔV [V]	f [Hz]	Vmax [V]	ΔV [V]	f [Hz]	Vmax [V]	ΔV [V]	ΔV [V]
CutsT0	0,00000	0,0	75,32	9,644	11,36	471,48	7,109	16,20	1320,01	8,736	15,26	42,81
				–1,714			–9,088			–6,520		
***T*1**	0,00031	1,0	71,67	9,574	11,28	431,56	8,109	18,11	1189,81	9,795	17,49	46,87
				–1,702			–9,997			–7,690		
***T*2**	0,00062	2,0	69,87	9,553	11,25	415,84	7,906	18,32	1138,70	10,397	18,00	47,57
				–1,700			–10,412			–7,605		
***T*3**	0,00093	3,0	68,33	9,522	11,22	402,76	7,701	18,45	1079,01	10,934	18,42	48,08
				–1,694			–10,744			–7,489		
***T*4**	0,00186	6,0	64,11	9,452	11,13	373,99	7,156	18,59	1007,12	12,307	19,37	49,10
				–1,681			–11,437			–7,064		
***T*5**	0,00279	9,0	60,68	9,424	11,10	354,59	6,719	18,52	949,83	13,271	19,85	49,48
				–1,677			–11,805			–6,580		
***T*6**	0,00372	12,0	57,82	9,364	11,03	340,60	6,347	18,33	911,29	13,905	20,01	49,37
				–1,665			–11,979			–6,109		
***T*7**	0,00558	18,0	53,21	9,299	10,95	321,95	12,122	17,96	865,88	14,550	19,89	48,80
				–1,652			–5,834			–5,339		
***T*8**	0,00744	24,0	49,85	9,226	10,87	310,76	12,077	17,56	843,71	14,634	19,43	47,85
				–1,640			–5,483			–4,794		
***T*9**	0,00930	30,0	47,41	9,177	10,81	304,37	11,956	17,20	834,00	14,499	18,94	46,94
				–1,629			–5,245			–4,436		
***T*10**	0,01116	36,0	44,67	9,126	10,75	301,72	11,826	16,87	831,75	14,249	18,46	46,08
				–1,621			–5,048			–4,211		
***T*11**	0,01302	42,0	43,02	9,083	10,70	302,63	11,687	16,56	834,75	13,922	18,00	45,25
				–1,612			–4,868			–4,074		
***T*12**	0,01488	48,0	41,53	9,066	10,68	307,30	11,535	16,21	842,48	13,585	17,54	44,43
				–1,609			–4,676			–3,958		
***T*13**	0,01801	58,1	39,37	9,063	10,67	321,20	11,141	13,99	873,42	12,935	16,49	41,16
				–1,609			–2,851			–3,559		
***T*14**	0,01990	64,2	38,40	9,259	10,91	320,53	10,948	13,66	901,88	12,619	15,00	39,57
				–1,655			–2,710			–2,379		

Finally are considered at the same time the contribution to the optimization of the second and the third vibration mode, with the configuration of the piezoelectric layer of the Energy Harvester that is shown in Fig. 3.11. The table 3.3 summarize the results of this simulation.

As shown in the table, the *Optimum Configuration is the "T5"*where the 9% of the total amount of piezoelectric material is removed and under this conditions the electrical

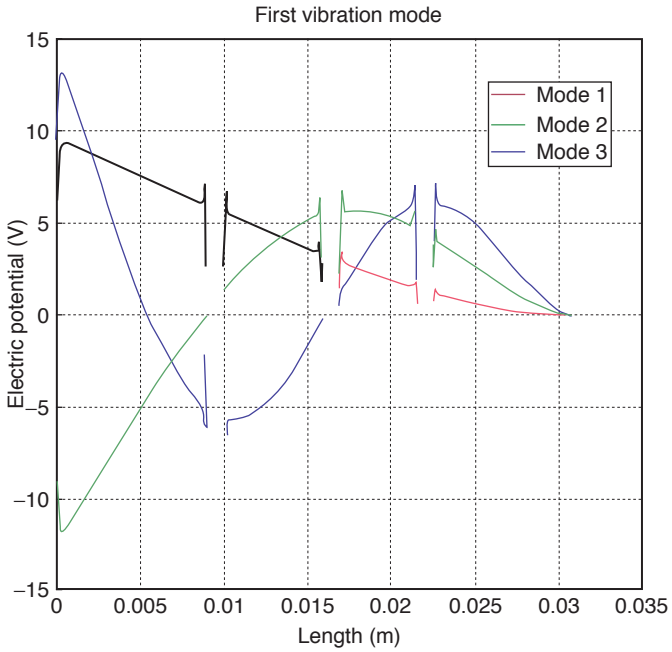

Figure 3.14

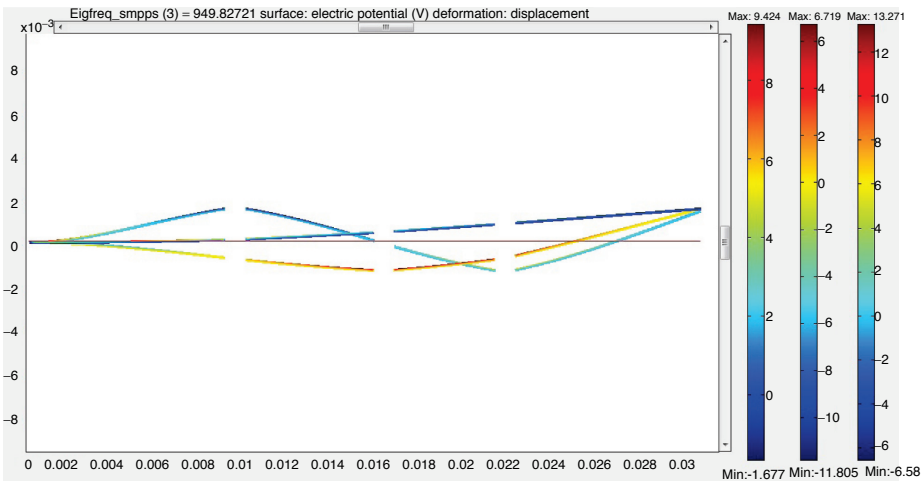

Figure 3.15

potential difference (ΔV) increases from 42,81V of the configuration "*T*0" to 49,48V of the "*T*5", the trend of theof the voltage in the *Global Optimum Configuration*, for the first three vibration modes is shown in Fig. 3.14 and the deformation shape for each mode in Fig. 3.15.

4. CONCLUSIONS

The produced voltage reaches the optimum under the highlighted conditions, proving that the optimized device is 16% more efficient when the amount of the removed material is the 9% of the total, but the table 3.3 shows that also for larger quantities of removed material, the device provides an Electrical Potential Difference that is better than the initial configuration, with the total piezoelectric layer without cuts in the material. This is true until the configuration "*T*12", with has the 48% of the piezoelectric material removed near the inflection points, which improves the efficiency of the device of a 3,78% compared with the initial configuration "*T*0".

ACKNOWLEDGMENTS

This research is supported by MIUR – Program PRIN 2009: "Model development and simulations based on the Finite Elements Method for ultrasound Non Destructive testing of industrial products".

REFERENCES

[1] A. Chandrakasan, R. Amirtharajah, J. Goodman, W. Rabiner, "Trends in low power digital signal processing", *Proceedings of the 1998 IEEE International Symposium on Circuits and Systems*, ISCAS, 98.

[2] C.B. Williams, R.B. Yates, "Analysis of a micro-electric generator for microsystems", *Sensors and Actuators A52 (1996)* 8–11.

[3] P. Glynn-Jones, S.P. Beeby, N.M. White, "Towards a piezoelectric vibration-powered microgenerator", *IEE Proceedings Science Measuring Technologies 148 (2001)* 69–72.

[4] Y.B. Jeon, R. Sood, J. Jeong, S. Kim, "MEMS power generator with transverse mode thin film PZT", *Sensor and Actuators A122 (2005)* 16–22.

[5] B. Zheng, C.-J. Chang, H. Chang Gea, "Topology optimization of energy harvesting devices using piezoelectric materials", *Struct. Multidisc. Optim. (2009)* 38:17–23.

[6] Metwally R. Emam, "Finite element analysis of composite piezoelectric beam using Comsol", *Thesis submitted to the Faculty of Drexel University, Master of Science in Mechanical Engineering, 2008*.

[7] A. Erturk, D.J. Inman, "*Piezoelectric energy harvesting*", a John Wiley and Sons, Ltd., Publication, United Kingdom, 2011.

[8] S. Lee, B.D. Youn, "A new piezoelectric energy harvesting design concept: multimodal energy harvesting skin", *IEEE transactions on ultrasonic, ferroelectrics and frequency control*, vol.58, No. 3, March 2011.

[9] An American National Standard, "IEEE standard on piezoelectricity – ANSI/IEEE Std 176–1987", *The institute of Electrical and Electronics Engineers, Inc*. New York, USA, 1988.

[10] H. Allik, T.J.R. Hughes, "Finite element method for piezoelectric vibration", *Int. Numerical Methods Engineering*, vol. 2, n. 2, 157–157, 1970.

BIOGRAPHY

Giuseppe Acciani received the M.Sc. degree (summa cum laude) in electrical engineering from the University of Bari, Bari, Italy, in 1981. After graduation, he had got a Grant at a Computer Research Centre (CSATA, Italy) attending to microprocessor interfacing. In 1985, he joined the Department Of Electrical And Computer Engineering of the Politecnico di Bari (Technical University), Italy, as an Assistant Professor, where he is currently an Associate Professor. At present, he is in charge of the following courses: "Electric Circuits," "Innovative Materialsfor Electrical Engineering," and "Intelligent Systems for Industrial Diagnostics." His main research interests concern the fields of photovoltaic plants monitoring, Energy Harvesting employing innovative materials and neural networks, in particular unsupervised networks for clustering, and soft computing for nondestructive diagnostics by means of ultrasonic waves and infrared techniques.

Antonietta Dimucci received the M.Sc. degree in Computer Engineering in March 2009 debating a degree thesis concerning the Matrix-Based discrete event control of mobile sensor networks, since January 2010 she is a PhD student in Electrical Engineering at Department Of Electrical And Computer Engineering of the Politecnico di Bari, Bari, Italy. Her main research interests concern the piezoelectric materials as functional materials in smart structures and energy harvesting. Her recent activity has been focused on the study and the optimization of energy harvesters and their modeling and analysis by means of finite-element method.

Leonardo Lorusso received the M.Sc. degree in Electrical Engineering in July 2012 debating a degree thesis concerning the Piezoelectric devices optimization for Energy Harvesting under the supervision of Prof. Acciani at the Politecnico di Bari, Bari, Italy. Actually collaborates with the research group of Electrical Engineering at the Department Of Electrical And Computer Engineering of the Politecnico di Bari.